Available online at www.sciencedirect.com
ScienceDirect
Journal of Nuclear Materials 367–370 (2007) 1590–1595
journal of nuclear materials
www.elsevier.com/locate/jnucmat

Liquid metal compatibility under irradiation: The LiSoR 5 experiment

H. Glasbrenner, F. Gröschel *

Paul Scherrer Institut, 5232 Villigen PSI, Switzerland

Abstract

LiSoR (liquid solid metal reaction) is a unique irradiation facility in which a specimen is exposed simultaneously to flowing liquid metal and a proton beam. The LiSoR loop and the test section were designed and constructed for irradiation with 72 MeV protons generated by PSI Philips cyclotron to investigate mainly the effect of liquid metal corrosion and embrittlement under irradiation onto the ferritic/martensitic steel T91. In the LiSoR 5 experiment the total beam current was 16.2 mA h and the irradiation dose on the specimen was about 0.75 dpa. Post irradiation examination (PIE) was carried out on the LiSoR specimen by means of SIMS, SEM/EDX and EPMA. The main result is the formation of a double layered oxide on the steel surface in the irradiated area. The maximum thickness of this layer is around 1.5 μm.

1. Introduction

Most future nuclear applications like lead-cooled fast reactors (LFR), accelerator driven systems (ADS) and fusion reactors are planned to use lead or lead alloy as coolant, breeder and/or spallation target material [1]. There is still a huge effort in development needed until such a device really can start to operate and generate power. One important point is the stability of the structural materials used which has to be guaranteed until the end of life. Because of this concern, the investigation of the behaviour of different structural materials in liquid Pb [2–4], Pb–17Li [4–8] and Pb–55.5Bi [3,4,9–13] has been performed for a long time. Procedures of examining and qualifying reactor materials for fusion are similar to ADS and LFR reactors and therefore a know-how transfer among the different research communities is useful to save resources and to increase their knowledge.

The MEGAPIE (1 MEGAwatt PIlot Experiment) project is aimed at designing, building and operating a liquid metal spallation neutron target as a key experiment on the road to an ADS reactor [14]. MEGAPIE will use lead bismuth eutectic (LBE) as the spallation material and the ferritic martensitic steel T91 as beam entrance window. LiSoR (liquid solid reaction) [15], a subproject of MEGAPIE, was launched to investigate the simultaneous influence of LBE and protons on T91 to investigate the behaviour of the steel under MEGAPIE relevant conditions. Up to now 5 tests were

* Corresponding author. Tel.: +41 56 310 4712; fax: +41 56 310 2199.
E-mail address: heike.glasbrenner@psi.ch (F. Gröschel).

0022-3115/$ - see front matter © 2007 Published by Elsevier B.V.
doi:10.1016/j.jnucmat.2007.04.036

performed and the results achieved on the irradiated T91 specimen from the latest experiment are presented in this paper.

2. Experimental

2.1. Material

The DIN 1.4903 steel 9Cr1MoVNb named T91 was supplied by the company CLI-FAFER (France) and has a composition in wt% of 8.41 Cr, 0.08 Ni, 0.95 Mo, 0.44 Mn, 0.31 Si, 0.1 C, 0.25 V, 0.08 Nb, 0.24 Si, 0.035 Cu, 0.002 S with the balance Fe. The material was delivered in standard heat treated condition, i.e. the steel was normalized at 1070 °C for 1 h followed by air cooling, and then tempered at 765 °C for 1 h followed by air cooling. The dimensions of the beam window and the test section are given in [15–17]. The loop and most of the test section were fabricated of AISI 316L steel.

2.2. LiSoR loop

The LiSoR (liquid solid reaction) loop is an experimental facility with an intermountable test section designed and constructed for operating during irradiation. It is installed in a bunker which is directly connected to a beam line from the PSI 72 MeV accelerator Injector 1. The loop operates fully automatically and is equipped with an electromagnetic pump, a flow meter and a heat exchanger system. The parts exposed to the proton beam are the beam window, the tensile specimen located in the tube and the flowing LBE. Details of the LiSoR loop can be found in previous reports [15,16].

2.3. Experimental conditions

The pre-heated LiSoR loop was filled with about 15 l of molten LBE from the storage tank up to a certain level that is controlled by six level sensors located in the test section. The loop with LiSoR test section no. 5 operated 1508 h during which the total time of irradiation was 724 h. It was decided that LiSoR loop would keep on running if there are longer periods of beam interrupts. The parameters of LiSoR 5 experiment are summarised in Table 1.

2.4. Post irradiation examination (PIE)

The dissembled test section no. 5 was transferred in a special transport flask to the PSI hot laboratory for dismantling and visual inspection. After a decay of 180 days the dose rate of the irradiated specimen was about 27 Sv/h on contact and 95 mSv/h at a distance of 10 cm. γ-mapping was carried out on the specimen after visual inspection and before cutting it into small samples for further analyses. The counts of ^{54}Mn, one of the main nuclides, having a half life time of 312.2 d were measured during the mapping to obtain the position and size of the irradiated area (see Fig. 1). ^{54}Mn is generated during irradiation from the steel elements Fe and Cr as a direct spallation product. The results of the

Table 1
Summary of the parameters of LiSoR 5 irradiation experiment

Parameter	Value
Beam energy on target	72 MeV
Maximum beam current	30 μA
Beam profile on target (Gaussian)	$\sigma_x = \sigma_y = 1.2$ mm
Beam wobbling max frequency	14 Hz in X, 2.33 Hz in Y (6:1)
Wobbling horizontal	$x_{max} = \pm 2.75$ mm
Wobbling vertical	$y_{max} = \pm 7$ mm
Time of irradiation	724 h
Total time of operation	1508 h
Flow rate in the test section	0.8 m/s
Temperature in LBE during irradiation[a]	360 °C
Temperature in LBE without irradiation[a]	300 °C
Temperature on the surface of specimen[b]	380 °C
Irradiation dose in specimen[b]	0.75 dpa
He concentration in specimen[b]	26 appm
Total current on LiSoR[b]	16.2 mA h

[a] Values directly measured during operation.
[b] Values calculated/estimated.

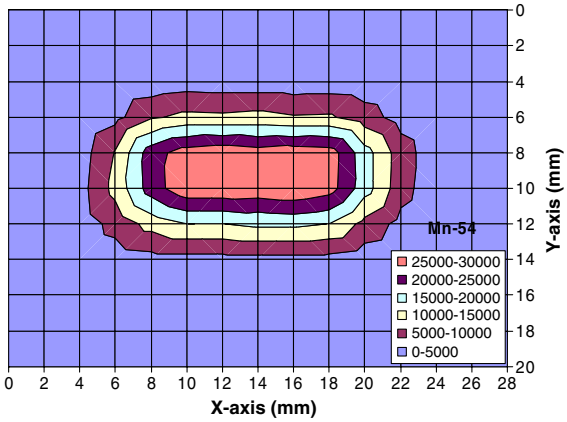

Fig. 1. γ-mapping of the specimen to detect precisely the irradiated area. The numbers are the count rates of ^{54}Mn measured in 20 min.

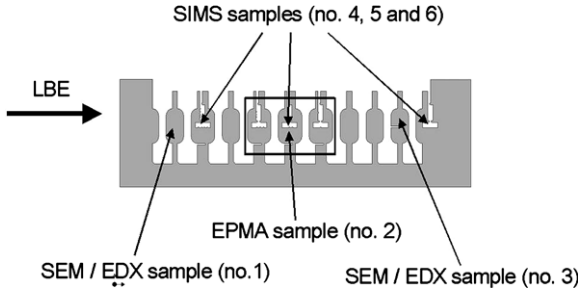

Fig. 2. Schematic of the cutting plan of the specimen including the position of the samples and the methods used for examination.

γ-mapping have been the basis for cutting the specimen by EDM wire cutting in a hot cell into samples for subsequent analyses. In Fig. 2 the schematic of the cutting plan includes the position of the irradiated area marked by a rectangle and the inspection method of each sample investigated. The surface has been examined by secondary ion mass spectrometry (SIMS), scanning electron microscopy (SEM), energy dispersive X-ray (EDX) analysis and electron probe micro analysis (EPMA) and the polished cross sectional cuts by SEM, EDX and EPMA. The irradiated area and also the adjacent areas were examined to compare the influence of irradiation. The dose rates of the samples examined, their position and number and the method chosen for analysis are summarised in Table 2.

Table 2
Dose rates and position of the samples examined with SEM, EDX, SIMS and EPMA

Sample no.	Analysis method	Dose rate (micro Sv/h) at 10 cm distance	Position of the specimen (0 = centre of the irradiated area)
1	SEM/EDX	<1	−22 mm
2	EPMA	5000	0
3	SEM/EDX	<1	+23 mm
4	SIMS	2	−18 mm
5	SIMS	1300	0
6	SIMS	<1	+ 29 mm

3. Results

3.1. Surface inspection (visual and with SEM/EDX)

The visual inspection of the T91 specimen showed the beam entrance and exit area: front and backside (Fig. 3(a) and (b)). The specimen is nearly completely covered with solidified LBE and the highest amount of residual sticking on the surface is found to be below the beam foot print. SEM performed on the surfaces of samples no. 1 and 3 showed that the specimen is widely covered with LBE and the steel surface is visible only in few areas of the specimen.

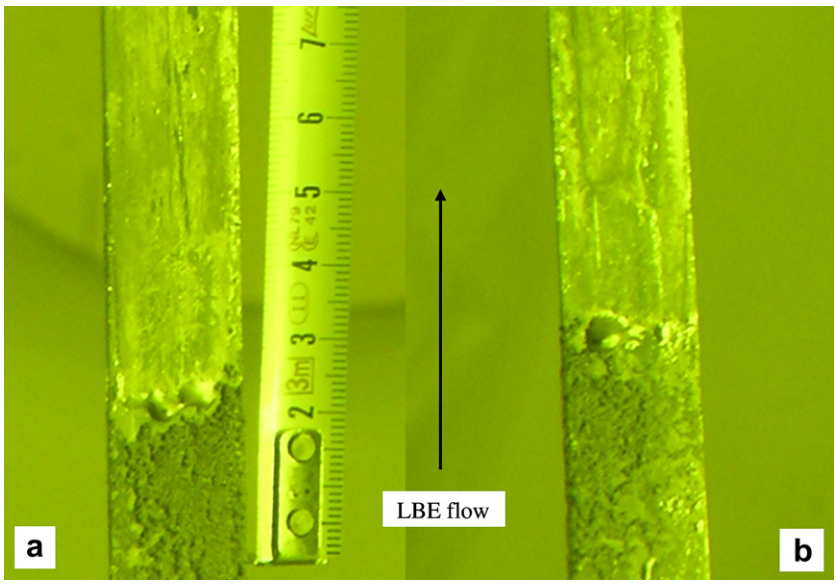

Fig. 3. Visual inspection of the irradiated specimen: (a) front and (b) back side.

3.2. SEM/EDX results (cross section)

The samples were embedded without any further cleaning step to avoid removing LBE. SEM/EDX inspections were carried out on sample no. 1 located below and on sample no. 3 located above the irradiated area, on polished cross sections from the front side and the backside. The dose rate of each sample, with less than 1 μSv/h measured at a distance of 10 cm, was relatively low and therefore they could be examined using the SEM of PSI hot lab (which is not a fully shielded device). In Fig. 4 the BSE (backscattering electron) images are presented in which (a) shows sample no. 1 and (b) sample no. 3. Similar observations were made on both samples: solidified LBE sticks on the sample surface. An interaction between steel and LBE is nowhere detected and in Fig. 4(a) a gap between the steel surface and the LBE confirms that no corrosion attack has occurred. A bi-structured layer of uniform thickness is visible on top of the steel surfaces. The total thickness is estimated to be about 1 μm. EDX point analysis and element distribution of Fe, Cr and O revealed the formation of a Fe_3O_4 layer on top and a $FeCr_2O_4$ layer staying in direct contact with the steel.

3.3. EPMA results (cross section)

Sample no. 2 was embedded and polished without previous removal of the adherent LBE. EPMA inspection was performed on the cross sectional cut including WDS analysis to obtain the chemical composition of the oxide layer plus the adherent LBE. At the top of the steel surface an oxide layer was detected having a maximum thickness of about 1.5 μm. The WDS analysis has confirmed the existence of the double layered oxide consisting of Fe_3O_4 on top and $FeCr_2O_4$ spinel in the intermediate.

3.4. SIMS results

SIMS spectra were measured on samples no. 4, 5 and 6 without removing adherent LBE from the surface. The measurements were performed by visual inspection on areas of the samples which were less or not at all covered with LBE. The SIMS spectrum obtained from the beam foot print (sample 5) is presented in Fig. 5. The outer layer consists mainly of Fe and O. The element Pb is present as well in this region but the other component of LBE, the element Bi, was not detected. The Cr content is negligible. In the intermediate region the Cr content increases, and the amount of Fe and O decreases slightly while the element Pb drops below the detection limit. These observations are in agreement with the results

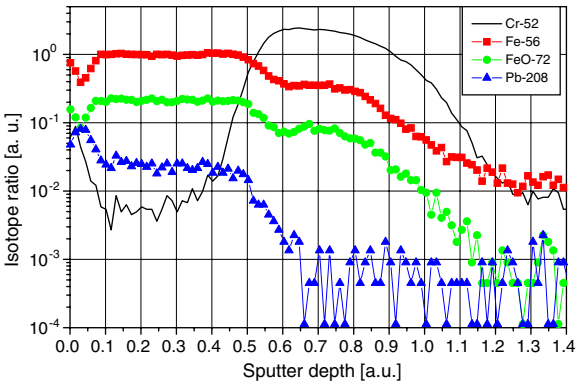

Fig. 5. SIMS spectra measured at the surface of the irradiated area clearly indicate the double structure of the oxide layer.

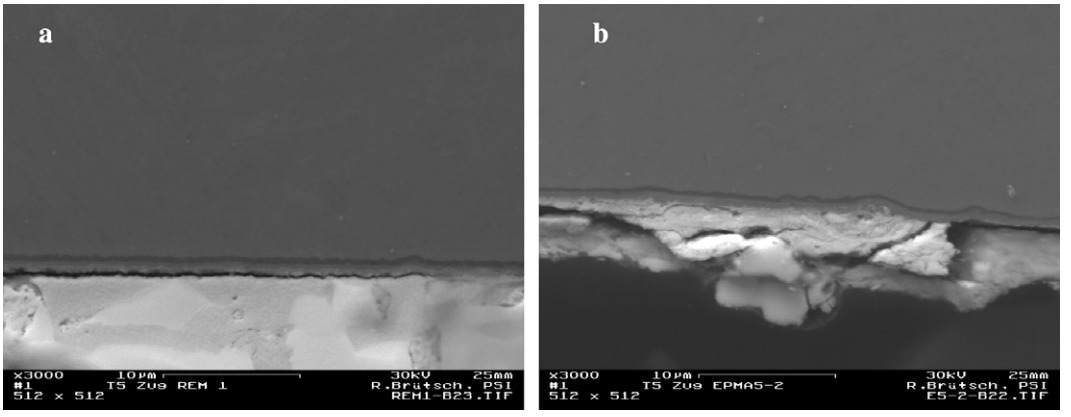

Fig. 4. SEM images of the cross sectional cut of the samples located (a) below (22 mm) and (b) above (23 mm) to the irradiated area.

presented above: an outer layer of Fe_3O_4 and an intermediate of $FeCr_2O_4$. The results achieved on the other two samples (no. 4 and 6) located adjacent to the irradiated area showed slightly thinner oxide layers but the same trend for the elements was detected.

4. Discussion and conclusion

The formation of a double structured oxide layer on the steel T91 was detected with different methods in the irradiated and as well in the adjacent areas. First of all it is fascinating that an oxide layer is generated in the beam foot print. The maximum thickness of the layer was reached in the irradiated area of about 1.5 μm and about 1 μm or less in the adjacent areas. The formation of oxide layers having the same chemical composition and structure was reported earlier on ferritic/martensitic steels staying in contact with oxygen saturated LBE [13,18–20].

The question to be answered is whether the growth of the oxide layer is just dependent on temperature, time and oxygen content in LBE or whether the neutrons and protons also influence the oxide growth on the steel. The oxide layers of LiSoR 5 have to be therefore compared with oxide layers formed under non-irradiated conditions in the same temperature range. The surface temperature of the T91 specimen in LiSoR 5 during irradiation was calculated to be 380 °C in the irradiated area [21], this means the specimen was exposed at 380 °C for 724 h (irradiation time) and to 300 °C for 784 h (time of operation of the loop). Most compatibility tests with T91 and LBE have been carried out at temperatures above 450 °C. Only in [13] results at 300 °C and in [18] at 400 °C are presented. Barbier and Rusanov [13] has observed no uniform corrosion effect for three different ferritic/martensitic steels including T91 after 3000 h of exposure at 300 °C. On some regions of the surface an oxide layer was detected. Being irregular in thickness it was not possible to evaluate its thickness.

Exposure tests of polished T91 at 350 °C in the PSI LBE loop CorrWett up to 6000 h have revealed a maximum thickness of the oxide layer of 2 μm after 6000 h, a thickness of about 800 nm after 1000 h and 1.5 μm after 3000 h of exposure [22]. The oxidation process of T91 follows a parabolic law [13,22] and is represented by the equation

$$d^2 = k_p t, \tag{1}$$

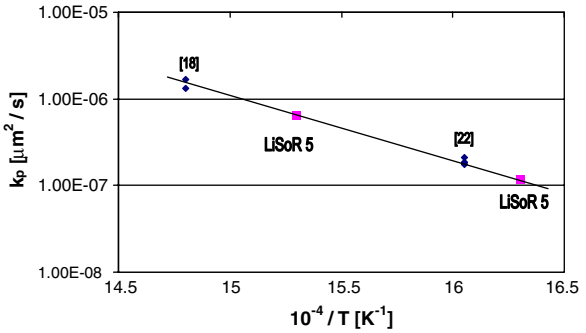

Fig. 6. Arrhenius plot of the parabolic rate constant as a function of the oxidation temperature.

where, d is the total thickness of the oxide layer, t is the oxidation time and k_p is the parabolic rate constant. Aiello et al. [18] have reported the formation of a 3 μm thick oxide layer after 1500 h of exposure at 400 °C in oxygen saturated LBE and 6 μm after 3000 h. These results are a bit surprising because they imply a linear corrosion rate. Further results are promised which hopefully will clarify this point. The values of [18] at 400 °C, of [22] at 350 °C and the LiSoR 5 at 380 °C and 340 °C (adjacent to the irradiated area) were used for calculating k_p. In Fig. 6 an Arrhenius plot of the parabolic rate constants as a function of the oxidation temperature is given. By taking the scattering of the thickness values into consideration the data are reasonably fitted by a straight line. The LiSoR value generated during irradiation is on the same line as the others which were produced in non-irradiated environments.

At first glance it seems that irradiation has no influence on the growth of the oxide layer. However, one has to keep in mind that the oxide layers are relatively thin in the temperature range of 300–400 °C and at maximum exposure times of 6000 h the scatter of the values is relatively large. Furthermore at 380 °C only one value was at hand for calculating the parabolic rate constant.

Further irradiation experiments on possible structural materials in the 'real' environment and under the 'real' conditions are required to understand what really happens. Under this point of view the relevance of well-planned irradiation experiments will gain in importance.

Acknowledgements

The authors wish to express their thanks for the assistance of D. Viol, K. Geissmann, R. Erne, P.

Meyer and O. Morath for their support of the irradiation experiment. The success of the PIE is the effort of V. Boutellier, M. Martin, R. Brütsch and R. Restani.

References

[1] J.R. Weeks, Nucl. Eng. Design 15 (1971) 363.
[2] H. Glasbrenner, J. Konys, G. Müller, A. Rusanov, J. Nucl. Mater 296 (2001) 237.
[3] C. Fazio, G. Benamati, C. Martini, G. Palombarini, J. Nucl. Mater. 296 (2001) 243.
[4] G. Ilincev, Nucl. Eng. Design 217 (2002) 167.
[5] G. Benamati, M. Agostini, I. Alessandrini, S. Storai, J. Nucl. Mater. 212–215 (1994) 1515.
[6] T. Flament, P. Tortorelli, V. Coen, H.U. Borgstedt, J. Nucl. Mater. 191–194 (1992) 132.
[7] H. Glasbrenner, J. Konys, Z. Voß, J. Nucl. Mater. 281 (2000) 225.
[8] J. Sannier, T. Dufrenoy, T. Flament, A. Terlain, J. Nucl. Mater. 191–194 (1992) 975.
[9] Y. Kurata, M. Futakawa, S. Saito, J. Nucl. Mater. 343 (2005) 333.
[10] M. Kondo, M. Takahashi, T. Suzuki, K. Ishikawa, K. Hata, S. Qiu, H. Sekimoto, J. Nucl. Mater. 343 (2005) 349.
[11] G. Müller, A. Heinzel, J. Konys, G. Schumacher, A. Weisenburger, F. Zimmermann, V. Engelko, A. Rusanov, V. Markov, J. Nucl. Mater. 335 (2004) 163.
[12] L. Soler, F.J. Martín, F. Hernández, D. Gómez-Briceño, J. Nucl. Mater. 335 (2004) 174.
[13] F. Barbier, A. Rusanov, J. Nucl. Mater 296 (2001) 231.
[14] F. Gröschel, J. Nucl. Mater. 335 (2004) 156.
[15] T. Kirchner et al., J. Nucl. Mater. 318 (2003) 70.
[16] S. Dementjev, H. Glasbrenner, T. Kirchner, F. Heinrich, I. Bucenieks, E. Platacis, A. Pozdnjaks, G. Kirshtein, Magnetohydrodynamics 37 (2001) 386.
[17] H. Glasbrenner, Y. Dai, F. Gröschel, J. Nucl. Mater. 343 (2005) 267.
[18] A. Aiello, M. Azzati, G. Benamati, A. Gessi, B. Long, G. Scaddozzo, J. Nucl. Mater. 335 (2004) 169.
[19] G. Müller et al., J. Nucl. Mater. 335 (2004) 163.
[20] D. Gomes Briceno, F.J. Martin Munoz, L. Soler Crespo, F. Estefan, C. Torres, J. Nucl. Mater. 296 (2001) 265.
[21] K. Samec, PSI Technical Report, TM-34-05-02, 2005.
[22] H. Glasbrenner, unpublished results.